

NUMERICAL SIMULATION OF WATER DRAINAGE IN DOUBLE-POROSITY SOILS

ADAM SZYMKIEWICZ*

Laboratoire d'étude des Transferts en Hydrologie et Environnement (LTHE),
UMR 5564 (CNRS, INPG, IRD, UJF). BP53, 38041 Grenoble Cedex 09, France.

Faculty of Civil Engineering and Environmental Engineering, Gdańsk University of Technology,
ul. Narutowicza 11/12, 80-952 Gdańsk, Poland.

JOLANTA LEWANDOWSKA, MICHEL VAUCLIN

Laboratoire d'étude des Transferts en Hydrologie et Environnement (LTHE),
UMR 5564 (CNRS, INPG, IRD, UJF). BP53, 38041 Grenoble Cedex 09, France.

KAZIMIERZ BURZYŃSKI

Faculty of Civil Engineering and Environmental Engineering, Gdańsk University of Technical,
ul. Narutowicza 11/12, 80-952 Gdańsk, Poland.

Abstract: The paper deals with modelling of unsaturated water flow in soils which are composed of two distinct sub-domains of very different hydraulic properties (double-porosity soils). Flow in such media is often characterized by the local non-equilibrium of the capillary pressure in the two regions, which cannot be described by the local equilibrium model [4]. Recently, a non-equilibrium model based on the homogenization approach has been proposed [5]. In the present paper, the model is applied to simulate gravitational drainage in a particular case of double-porosity medium. The medium consists of highly conductive sand matrix with weakly conductive spherical inclusions arranged in a periodic manner. The numerical simulations have been performed with the DPOR-1D code [11]. Calculation of the effective parameters of the medium is presented as well as the solution of the macroscopic boundary value problem. The behaviour of the double-porosity medium is compared with the behaviour of single-porosity media, i.e. a homogeneous sand and a sand with impermeable inclusions. The results show the importance of the non-equilibrium effects for the flow in double-porosity soils.

NOTATION

Physical units: L – length, M – mass, T – time.

Indices 1 and 2 refer to the matrix and inclusions, respectively.

LATIN LETTERS

- C – specific water capacity [L^{-1}].
 C^{eff} – effective water capacity [L^{-1}].
 h – macroscopic capillary pressure head [L].

* Corresponding author: email: adams@ibwpan.gda.pl; now at: Institute of Hydroengineering of the Polish Academy of Sciences, ul. Kościarska 7, 80-953 Gdańsk, Poland.

h_2	– capillary pressure head in inclusions [L].
\mathbf{I}	– identity matrix.
\mathbf{K}_1	– hydraulic conductivity tensor of the matrix [LT ⁻¹].
\mathbf{K}^{eff}	– effective hydraulic conductivity tensor [LT ⁻¹].
K_S	– hydraulic conductivity at saturation [LT ⁻¹].
m	– water retention function parameter (van Genuchten–Mualem model), $m = 1 - 1/n$ [–].
\mathbf{N}	– unit vector normal to the interface Γ .
n	– water retention function parameter (van Genuchten–Mualem model) [–].
t	– time [T].
w_1, w_2	– volumetric fractions of the matrix and the inclusions [–].
\mathbf{X}	– macroscopic space coordinate [L].
\mathbf{Y}	– local space coordinate [L].

GREEK LETTERS

α	– water retention function parameter (van Genuchten–Mualem model) [L ⁻¹].
Γ	– interface between media 1 and 2.
θ_R	– residual volumetric water content (van Genuchten–Mualem model) [–].
θ_S	– saturated volumetric water content (van Genuchten–Mualem model) [–].
χ	– vector function, solution of the local boundary value problem [–].
Ω	– period domain.
Ω_1, Ω_2	– sub-domains of the period occupied by media 1 and 2.

1. INTRODUCTION

Double-porosity soils are highly heterogeneous media, characterized by the presence of two distinct porous sub-domains with contrasting hydraulic parameters. For example, in aggregated soils one sub-domain can be associated with weakly conductive soil aggregates, while the other sub-domain corresponds to the inter-aggregate space filled with coarser, highly conductive material. The time required to equilibrate the capillary pressure is very different in each region. Due to this particular structure local non-equilibrium conditions often arise during the water flow. The non-equilibrium effects cannot be described using the single-porosity model presented in [4]. A number of different empirical approaches to model non-equilibrium flow in unsaturated soils have been developed, see [10] for an extensive review.

Recently, a model of non-equilibrium flow has been proposed by LEWANDOWSKA et al. [5]. The authors used the homogenization technique [1], [3], [9] to derive the macroscopic model in a mathematically rigorous manner. The model has been implemented in the DPOR-1D numerical code [11]. The aim of this paper is to provide an illustrative example of the application of this model. In contrast to the previous contribution [5], our attention is focussed on the qualitative and quantitative comparison of the behaviour of double- and single-porosity media during gravitational drainage.

2. THEORETICAL MODEL

The macroscopic model [5] was derived for a periodic medium (the period domain being denoted by Ω), which is composed of a highly conductive interconnected matrix Ω_1 and a weakly conductive inclusions Ω_2 with the interface Γ between the two sub-domains. It has the form of the following single integro-differential nonlinear equation [5]:

$$C^{\text{eff}} \frac{\partial h}{\partial t} - \frac{\partial}{\partial X_i} \left[K_{ij}^{\text{eff}} \left(\frac{\partial h}{\partial X_j} - I_{j3} \right) \right] + \frac{1}{|\Omega|} \int_{\Omega_2} C_2 \frac{\partial h_2}{\partial t} d\Omega = 0, \quad (1)$$

where h [L] is the macroscopic capillary pressure head ($h \leq 0$), $C^{\text{eff}}(h)$ [L^{-1}] is the effective water capacity, $\mathbf{K}^{\text{eff}}(h)$ [LT^{-1}] is the effective hydraulic conductivity tensor, h_2 [L] and $C_2(h_2)$ [L^{-1}] are the local capillary pressure head in the inclusions Ω_2 and the corresponding specific water capacity, respectively, X [L] is the spatial coordinate (X_3 axis being oriented positively downward) and t [T] is time. The integral term in eq. (1):

$$Q = \frac{1}{|\Omega|} \int_{\Omega_2} C_2 \frac{\partial h_2}{\partial t} d\Omega \quad (2)$$

represents the water exchange between the matrix sub-domain Ω_1 and the inclusions Ω_2 . It can be calculated by solving the additional local flow equation representing the inside of the inclusion at each point of the macroscopic domain:

$$C_2 \frac{\partial h_2}{\partial t} - \frac{\partial}{\partial Y_i} \left(K_{2ij} \frac{\partial h_2}{\partial Y_j} \right) = 0, \quad i, j = 1, 2, 3 \text{ in } \Omega_2 \quad (3)$$

with the pressure continuity condition at the interface Γ :

$$h_2 = h \quad \text{on } \Gamma. \quad (4)$$

In eq. (3), Y [L] is the local spatial coordinate associated with a single period, and $K_2(h_2)$ [LT^{-1}] is the local hydraulic conductivity of the inclusions.

If we assume that both sub-domains are locally homogeneous and isotropic, then the effective parameters are defined as follows [5]:

$$C^{\text{eff}}(h) = w_1 C_1(h), \quad (5)$$

$$K_{ij}^{\text{eff}}(h) = K_1(h) \frac{1}{|\Omega|} \int_{\Omega_1} \left(\frac{\partial \chi_j}{\partial Y_i} + I_{ij} \right) d\Omega, \quad i, j = 1, 2, 3, \quad (6)$$

where K_1 is the local hydraulic conductivity in the matrix sub-domain Ω_1 and the vector function χ is obtained from the solution of the following local boundary value

problem in a single period:

$$\frac{\partial}{\partial Y_i} \left[\left(I_{ij} + \frac{\partial \chi_j}{\partial Y_i} \right) \right] = 0, \quad i, j = 1, 2, 3 \text{ in } \Omega_1, \quad (7)$$

$$\left(I_{ij} + \frac{\partial \chi_j}{\partial Y_i} \right) N_i = 0 \quad i, j = 1, 2, 3 \text{ on } \Gamma, \quad (8)$$

where \mathbf{N} is the unit vector normal to Γ . Moreover, χ should be Ω -periodic and its volume average over Ω should be zero.

3. SOLUTION OF A DRAINAGE PROBLEM IN A DOUBLE-POROSITY MEDIUM

3.1. GEOMETRY, MATERIAL PROPERTIES AND BOUNDARY CONDITIONS

The numerical example concerns a drainage process in a 240-cm thick layer of a double-porosity medium. The medium is composed of highly conductive sand matrix with weakly conductive spherical inclusions (sintered clayey material). The spheres (0.64 cm in diameter) are arranged periodically as shown in figure 1a. The volume fraction of the matrix and inclusions are $w_1 = 0.445$ and $w_2 = 0.555$, respectively.

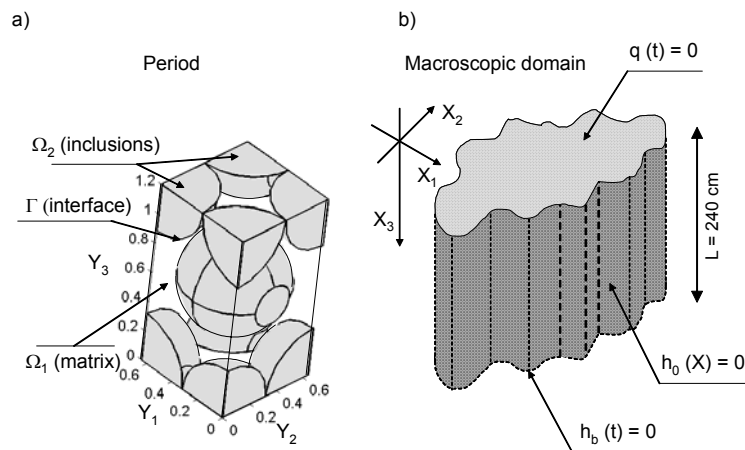


Fig. 1. Period geometry used in numerical example. Dimensions are in [cm] (a). Initial and boundary conditions for the macroscopic problem (b)

The hydraulic characteristics of the two porous materials are described by

Mualem–van Genuchten functions [7], [12] of the following form:

$$\theta(h) = \theta_R + (\theta_S - \theta_R)[1 + (\alpha|h|)^n]^{-m}, \quad (9)$$

$$K(h) = K_S[1 - (\alpha|h|)^{n-1}[1 + (\alpha|h|)^n]^{-m}]^2[1 + (\alpha|h|)^n]^{-m/2} \quad (10)$$

with $m = 1 - 1/n$. The values of the parameters for the sand matrix are: $\theta_R = 0.0$, $\theta_S = 0.342$, $\alpha = 1.38 \times 10^{-2} \text{ cm}^{-1}$, $n = 4.056$, $K_S = 2.83 \times 10^{-3} \text{ cm s}^{-1}$ and for the inclusions: $\theta_R = 0.0$, $\theta_S = 0.295$, $\alpha = 6.05 \times 10^{-3} \text{ cm}^{-1}$, $n = 2.269$, $K_S = 1.15 \times 10^{-9} \text{ cm s}^{-1}$. The values are taken from [6], except for K_S in inclusions, which has been reduced by 4 orders of magnitude. The retention and conductivity curves of the two materials are shown in figure 2.

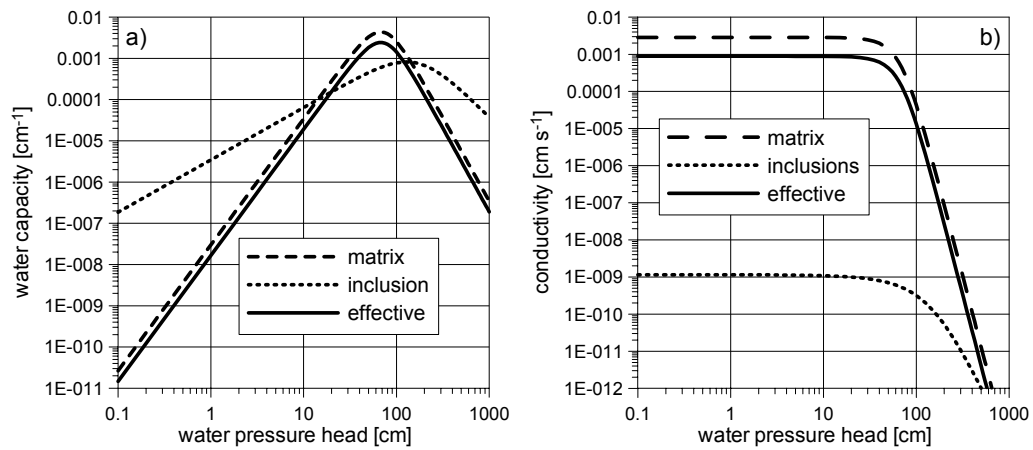


Fig. 2. Hydraulic properties of matrix, inclusions and double-porosity medium: a) specific water capacity, b) hydraulic conductivity

At macroscopic scale the flow is considered as one-dimensional. The initial and boundary conditions represent gravitational drainage of initially saturated layer:

- $h(X_3) = 0$ for $t = 0$ (full saturation),
- $q(t) = 0$ for $X_3 = 0$ (impermeable boundary at the surface),
- $h(t) = 0$ for $X_3 = 240 \text{ cm}$ (constant water level at the bottom of the layer, i.e. a depression of -240 cm with respect to the upper level).

3.2. CALCULATION OF THE EFFECTIVE PARAMETERS

According to eq. (5) the effective water capacity is given by the following formula: $C^{\text{eff}}(h) = 0.445 C_1(h)$. In order to determine the effective conductivity, one has to solve the following local boundary value problem for χ_3 :

$$\frac{\partial}{\partial Y_1} \left(\frac{\partial \chi_3}{\partial Y_1} \right) + \frac{\partial}{\partial Y_2} \left(\frac{\partial \chi_3}{\partial Y_2} \right) + \frac{\partial}{\partial Y_3} \left(1 + \frac{\partial \chi_3}{\partial Y_3} \right) = 0 \quad \text{in } \Omega_1, \quad (11)$$

$$\left(\frac{\partial \chi_3}{\partial Y_1} \right) N_1 + \left(\frac{\partial \chi_3}{\partial Y_2} \right) N_2 + \left(1 + \frac{\partial \chi_3}{\partial Y_3} \right) N_3 = 0 \quad \text{on } \Gamma. \quad (12)$$

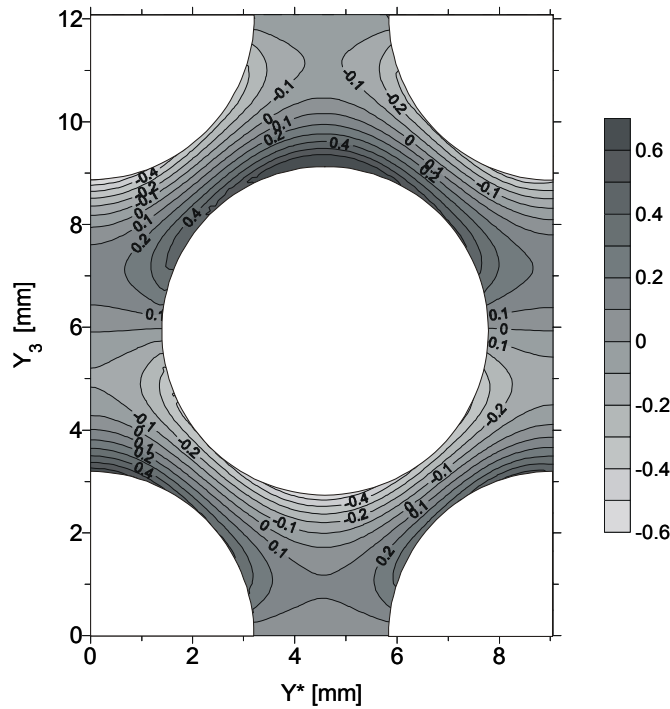


Fig. 3. Solution of the local boundary value problem – distribution of the χ_3 function.
The horizontal axis Y^* corresponds to the diagonal of the base of the parallelepiped ($Y_1 = Y_2$)

The solution was obtained using the DPOR-1D code. In figure 3, the distribution of the corresponding χ_3 function is presented in a diagonal cross-section plane of the period. After application of the definition of K_{33}^{eff} :

$$K_{33}^{\text{eff}}(h) = K_1(h) \frac{1}{|\Omega|} \int_{\Omega_1} \left(\frac{\partial \chi_3}{\partial Y_3} + 1 \right) d\Omega \quad (13)$$

the following relation between the effective conductivity and matrix conductivity was obtained: $K_{33}^{\text{eff}}(h) = 0.308 K_1(h)$. The effective parameters of the double-porosity medium are presented in figure 2.

3.4. SOLUTION OF THE MACROSCOPIC EQUATION

One-dimensional form of the macroscopic equation is the following:

$$C^{\text{eff}} \frac{h}{t} - \frac{\partial}{\partial X_3} \left[K_{33}^{\text{eff}} \left(\frac{\partial h}{\partial X_3} - 1 \right) \right] + Q = 0. \quad (14)$$

Equation (14) was solved using DPOR-1D code. The algorithm is based on an implicit finite difference approximation of eq. (1). The solution was obtained with the following numerical parameters: $\Delta X = 0.5$ cm (481 nodes), $\Delta Y = 0.032$ cm, $\Delta t = 10^{-6}$ s to 10^4 s, accuracy $\Delta h = 0.1$ cm.

4. RESULTS AND DISCUSSION

In order to show the difference in the behaviour of double- and single-porosity media, additional numerical simulations were carried out for a homogeneous medium (sand only) and a medium composed of sand matrix with impermeable inclusions.

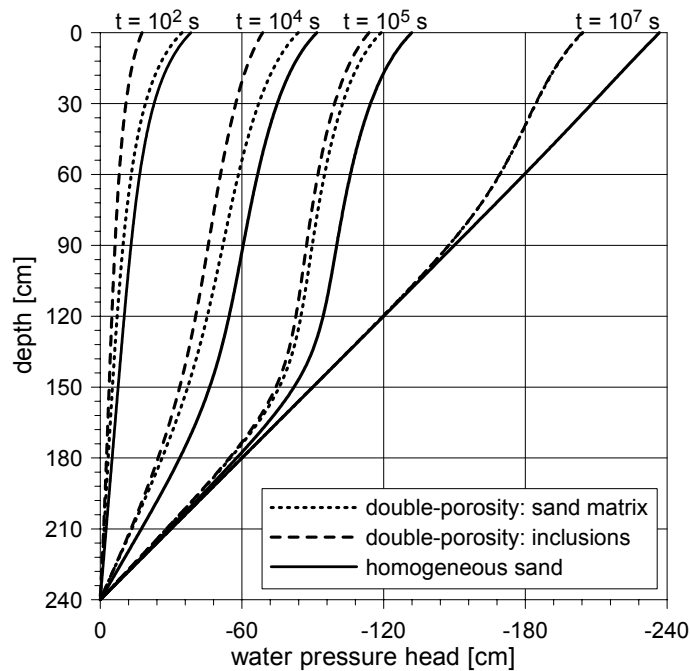


Fig. 4. Profiles of water pressure head in the double-porosity medium and in the homogeneous sand. For the double-porosity medium the values for the two sub-domains (sand matrix and inclusions) are shown separately

The results of the simulations are presented in figures 4–6. In figure 4, the profiles of pressure head along the column are shown for selected time levels. The results obtained for homogeneous sand are compared to those obtained for double-porosity medium. In the latter case, two separate profiles are shown: one for the macroscopic pressure head h (sand matrix) and one for the water pressure head averaged within the inclusions h_2 .

At the beginning the pressure head is close to zero (full saturation), and as the drainage continues the profiles approach the hydrostatic distribution with the value 0 at the bottom and -240 cm at the top of the layer. The drainage is much faster in homogeneous sand, while in case of double-porosity medium a considerable amount of water is stored in the inclusions, which drain very slowly. In the double-porosity medium, non-equilibrium of the pressure head between matrix and inclusions can be clearly seen. The difference between h and averaged h_2 is relatively large at the beginning of the drainage, and becomes smaller and smaller with time. After about 10^7 s the equilibrium is reached between the two sub-domains. However, even for that time, the hydrostatic distribution of pressure is not reached in the double-porosity medium.

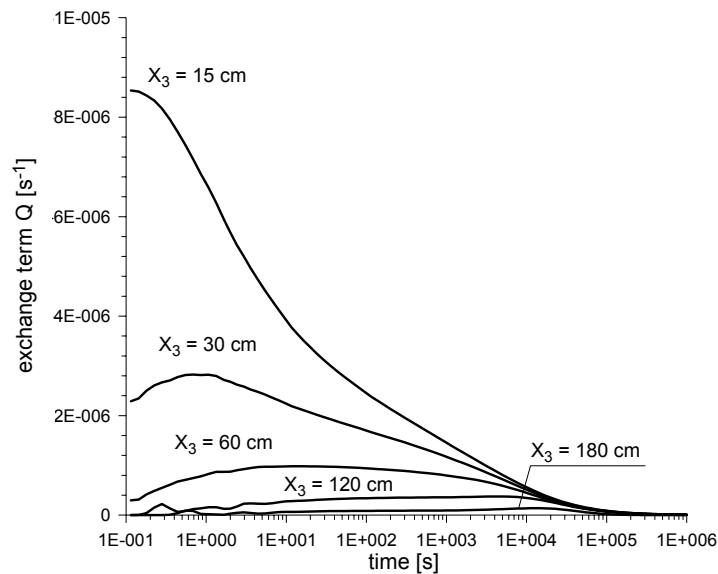


Fig. 5. Evolution of the exchange term Q (eq. (2)) at different depths of the soil layer

The intensity of water exchange between inclusions and sand matrix, represented by the non-equilibrium term, is shown in figure 5. Time evolution of this term is presented for different depths. The largest values occur at the beginning of the process in the upper part of the layer. As can be seen from figure 4, they correspond to the largest differences in the pressure head between the two sub-domains.

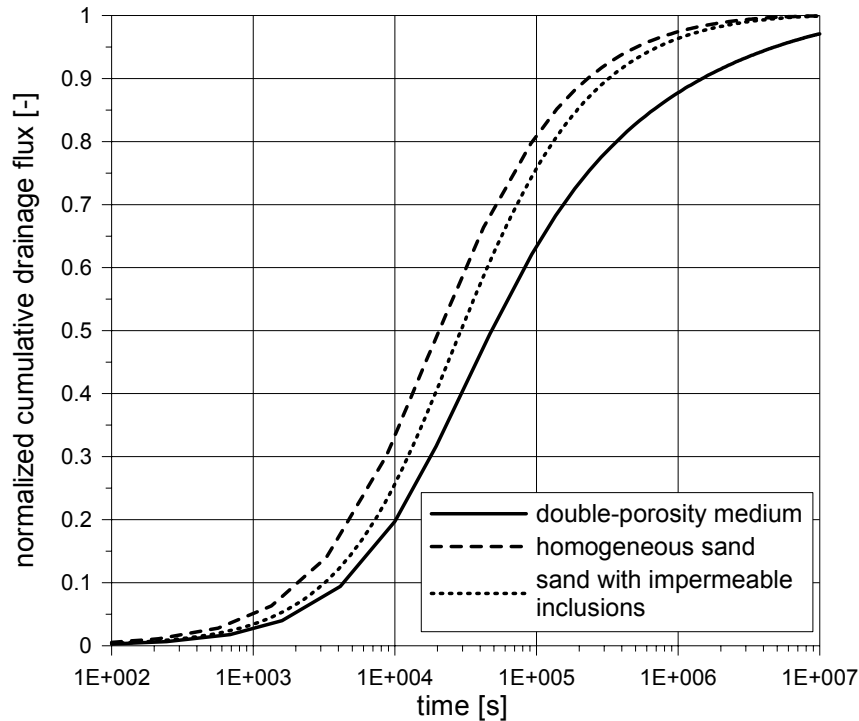


Fig. 6. Normalized cumulative drainage flux for the double-porosity medium, the homogenous sand and the sand with impermeable inclusions. The normalized cumulative drainage flux represents the quantity of drained water as a fraction of the total amount of water accessible for drainage in each medium

Figure 6 presents a comparison of macroscopic behaviour of the double-porosity medium with the homogeneous sand and the sand with impermeable inclusions. The normalized cumulative flux at the bottom of the layer is shown as a function of time. It represents the quantity of water obtained from drainage as a fraction of the total accessible amount of water for each medium. The three media behave differently. The drainage is the fastest in the homogeneous sand. In the medium with impermeable inclusions, the flow is slowed down in the initial phase. Both single-porosity media become completely drained after about 10^6 s. In contrast, the process is not completed in double-porosity medium even after 10^7 s due to the influence of weakly conductive inclusions.

5. CONCLUDING REMARKS

According to the results of the homogenization procedure the flow in double-porosity medium composed of a highly conductive matrix and weakly conductive inclusions can be described by a single macroscopic equation with two effective pa-

rameters. The local non-equilibrium of pressure caused by the presence of inclusions is taken into account by an integral term in the macroscopic equation. The numerical experiments performed here show the importance of the local non-equilibrium effects for the drainage flow. Generally, the flow is retarded in the double-porosity medium with respect to the single-porosity one due to the exchange of water between the matrix and the inclusions. Although those effects seem to be quantitatively smaller for the drainage case with respect to the infiltration case shown in [5], the macroscopic behaviour of the medium cannot be correctly represented by a single-porosity model.

REFERENCES

- [1] AURIAULT J.-L., *Heterogeneous medium: Is an equivalent macroscopic description possible?* Int. J. Engng Sci., 1991, Vol. 29, No. 7, pp. 785–795.
- [2] BEAR J., *Dynamics of Fluids in Porous Media*, Elsevier, 1972.
- [3] BENSOUSSAN A., LIONS J.-L., PAPANICOLAOU G., *Asymptotic analysis for periodic structures*, North-Holland, 1978.
- [4] LEWANDOWSKA J., LAURENT J.-P., *Homogenization modeling and parametric study of moisture transfer in an unsaturated heterogeneous porous medium*, Transport in Porous Media, 2001, Vol. 45, pp. 321–345.
- [5] LEWANDOWSKA J., SZYMKIEWICZ A., BURZYŃSKI K., VAUCLIN M., *Modeling of unsaturated water flow in double porosity soils by the homogenization approach*, Advances in Water Resources, 2004, Vol. 27, No. 3, pp. 283–296.
- [6] LEWANDOWSKA J., SZYMKIEWICZ A., GORCZEWSKA W., VAUCLIN M., *Infiltration in a double-porosity medium: experiments and comparison with a theoretical model*, Water Resources Research, accepted for publication, 2004.
- [7] MUALEM Y., *A new model for predicting the hydraulic conductivity of unsaturated porous media*, Water Resources Research, 1976, Vol. 12, No. 3, pp. 513–522.
- [8] RICHARDS L. A., *Capillary conduction of liquids through porous medium*, Physics, 1931, Vol. 1, pp. 318–333.
- [9] SANCHEZ-PALENCIA E., *Non-homogeneous media and vibration theory*, Lecture Note in Physics, 1980, Vol. 127, Springer-Verlag, Berlin.
- [10] ŠIMŮNEK J., JARVIS N. J., VAN GENUCHTEN M.TH., GÄRDENÄS A., *Review and comparison of models for describing non-equilibrium and preferential flow and transport in the vadose zone*, Journal of Hydrology, 2003, Vol. 272, pp. 14–35.
- [11] SZYMKIEWICZ A., *Modeling of unsaturated water flow in highly heterogeneous soils*, PhD dissertation, Université Joseph Fourier, Grenoble, Gdańsk University of Technology, 2004.
- [12] VAN GENUCHTEN M.TH., *A closed form equation for predicting the hydraulic conductivity of unsaturated soils*, Soil Science Society of America Journal, 1980, Vol. 44, pp. 892–898.